*Review*

# Primary Processes of Free Radical Formation in Pharmaceutical Formulations of Therapeutic Proteins

Christian Schöneich [ID]

Department of Pharmaceutical Chemistry, University of Kansas, 2093 Constant Avenue, Lawrence, KS 66047, USA; schoneic@ku.edu; Tel.: +1-(785)-864-4880

**Abstract:** Oxidation represents a major pathway for the chemical degradation of pharmaceutical formulations. Few specific details are available on the mechanisms that trigger oxidation reactions in these formulations, specifically with respect to the formation of free radicals. Hence, these mechanisms must be formulated based on information on impurities and stress factors resulting from manufacturing, transportation and storage. In more detail, this article focusses on autoxidation, metal-catalyzed oxidation, photo-degradation and radicals generated from cavitation as a result of mechanical stress. Emphasis is placed on probable rather than theoretically possible pathways.

**Keywords:** autoxidation; Fenton reaction; free radicals; mechanisms; oxidation; photo-degradation; cavitation

## 1. Introduction

The advent of biotechnology has enabled the production of recombinant proteins for therapeutic applications. A recent review of the globally highest-selling drugs in 2019 showed that out of ten drug products, seven were proteins [1]. Despite the therapeutic and commercial success of protein therapeutics, the development of stable protein formulations can present challenges [2–7]. Proteins are subject to physical and chemical degradation, potentially compromising the efficacy and safety of drug products. The physical degradation of proteins is often associated with processes such as surface adsorption, aggregation, particle formation and precipitation, while chemical degradation describes the covalent modification of amino acids. Frequently, the physical and chemical degradation of proteins are connected, where, for example, chemical modifications may trigger aggregation or conformational transitions of proteins may facilitate the accrual of chemical modifications.

Oxidation represents a major pathway for the chemical degradation of proteins, which can be carried out by a range of reactive oxygen and nitrogen species, including free radicals [8,9]. The field of redox biology presents many examples of proteins that are subject to oxidative modification in vivo under conditions of oxidative stress. These oxidative modifications may either result in no change in activity, or promote loss or gain of function, depending on the nature of the modifications and the specific proteins. Whether some of these oxidative modifications may be useful as clinical biomarkers will depend on the type, stability and location of the modifications and the pathologies of concern [10–12]. For example, commonly measured protein oxidation products such as protein carbonyls, methionine sulfoxide (MetSO) and some tyrosine-derivatives were poor biomarkers in the biological fluids of rats for either carbon tetrachloride ($CCl_4$)- or ozone-induced oxidative stress [13,14]. In contrast, some lipid-derived oxidation products, such as malondialdehyde (MDA) or isoprostanes, appeared to be viable biomarkers for $CCl_4$-induced oxidative stress in rats [13].

Many of the protein oxidation products that have been characterized in vivo can also form as a result of oxidative processes in therapeutic protein formulations in vitro [15]. In addition, these oxidation processes can generate a range of oxidation products from excipients, e.g., from amino acids, especially histidine (His) [16–19], and surfactants [18–24],

and likely also carbohydrates. Some of these oxidation products in vitro may correlate with important characteristics of their respective drug products, and are referred to as critical quality attributes (CQAs). For example, oxidation products may have consequences for the shelf-life, bioavailability or immunogenicity of drug products.

The exact nature and sources of oxidants in protein formulations are generally less well defined. For comparison, the biological mechanisms of oxidant production frequently rely on relatively well-characterized enzymes such as xanthine oxidase [25], nitric oxide synthase [26], myeloperoxidase [27] or NADPH oxidase [28]. In contrast, oxidation reactions in therapeutic protein formulations in vitro rely predominantly on adventitious processes promoted by, e.g., mechanical stress, impurities and/or exposure to elevated temperature, light or ionizing radiation. Details on the primary processes that lead to free radical formation and oxidation in pharmaceutical formulations would be highly valuable for the development of mitigation strategies. It is possible to outline the mechanisms of free radical generation in pharmaceutical formulations based on information on impurities and known stress factors that are relevant to pharmaceutical manufacturing, transportation and storage. This is the purpose of this article.

## 2. Composition of Pharmaceutical Formulations of Therapeutic Proteins

The pharmaceutical formulations of therapeutic proteins display a range of compositions for liquid, frozen and lyophilized forms. Relevant to the potential formation mechanisms of radicals is the fact that these formulations can generally contain several classes of compounds in addition to the protein, such as buffers, surfactants, amino acids, cryoprotectants, chelators and additional tonicifiers [1,29]. Besides the intended functions in the formulations, each of these respective components may play a role in free radical generation through its chemical properties and/or impurities, which may be introduced via chemical synthesis, purification and/or storage.

## 3. Pathways of Free Radical Formation That Are Relevant to Pharmaceutical Formulations

The following sections will discuss specific pathways of free radical generation with respect to the potential role of impurities and stress factors.

### 3.1. Autoxidation

Miller et al. define true autoxidation "as the spontaneous oxidation in air of a substance not requiring catalysts" [30]. Hence, autoxidation can be represented by the general reaction (1), where $D^-$ and $O_2^{\bullet-}$ represent an electron donor and superoxide, respectively, and $k_1$ and $k_{-1}$ are the rate constants for forward and reverse electron transfer.

$$D^- + O_2 \rightleftharpoons D^\bullet + O_2^{\bullet-} \qquad (1)$$

A plot of log $k_1$ vs. log $K_1$ (where $K_1$ represents the equilibrium constant for redox equilibrium 1) yields a curve that can be fitted to the Marcus equation, where $D^-$ represents a series of phenolates, indophenolates and other electron donors [31]. This relationship allows us to make an estimate of the sensitivity of amino acid side chains towards autoxidation on the basis of their reduction potentials. Such an estimate suggests that at most cysteine in its deprotonated form, with $E^o_2 \approx 0.75$ V for redox equilibrium 2 [32,33], would be susceptible to autoxidation at pH values generally selected for protein formulations.

$$RS^\bullet + e^- \rightleftharpoons RS^- \qquad (2)$$

This would limit autoxidation processes to proteins that contain free cysteine residues. Monoclonal antibodies do not contain free cysteine residues, except for small quantities of incompletely folded proteins, implying that autoxidation should be a negligible problem for pharmaceutical formulations containing monoclonal antibodies.

A second target for potential autoxidation would be surfactants [34], especially polysorbate 80, which contains oleic, linoleic and linolenic acid [35,36]. It is possible that autoxidation contributes to the generation of polysorbate radicals [37] and polysorbate oxidation products, including peroxides, in neat polysorbate [38]. However, it is equally likely that oxidation in neat polysorbate is triggered by the homolytic decomposition of reactive fatty acid:oxygen copolymers of the general structure **1** (Figure 1, where residues $R_n$, n = 1–6, depict moieties of fatty acids that have undergone successive peroxyl radical and oxygen addition to double bonds) [39,40], containing $\alpha,\beta$-diperoxide repeats analogous to styrene:oxygen copolymers [41]. Such fatty acid:oxygen copolymers may be generated during polysorbate synthesis and storage.
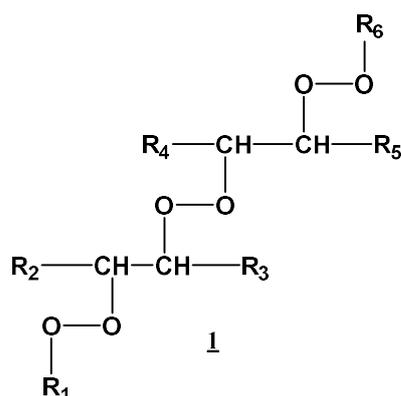


**Figure 1.** General structure of fatty acid:oxygen copolymers (Residues $R_n$, n = 1–6, depict moieties of fatty acids that have undergone successive peroxyl radical and oxygen addition to double bonds).

Morita and Tokita reported that fatty acid:oxygen copolymers are stronger initiators of lipid peroxidation in model experiments compared to simple hydroperoxides [39]. However, the fact that Bensaid et al. [42] observed that iron levels as low as 20 ppb accelerated polysorbate oxidation in aqueous formulations suggests that, at least in pharmaceutical formulations, metal-catalyzed reactions of hydroperoxides may be kinetically more significant for the formation of free radicals compared to metal-independent decomposition reactions of fatty acid:oxygen copolymers or autoxidation. This is also consistent with data showing the accelerated decomposition of polysorbate when in contact with stainless steel surfaces [19,43]. It is, therefore, unlikely that true autoxidation processes contribute significantly to free radical formation in pharmaceutical formulations.

*3.2. Fenton and Fenton-like Reactions between Metals and Peroxides*

Fenton and Fenton-like reactions represent important pathways for free radical generation. Peroxides can be introduced into formulations through excipients [44], primarily surfactants [38,44,45], and/or as a result of sterilization procedures [46]. Before presenting a detailed discussion of the potential radical-generating reactions of metals and peroxides in pharmaceutical formulations, we need to evaluate which metals and which reactions are most relevant to pharmaceutical formulations. The International Council for Harmonization (ICH) Q3D(R2) guidelines define three classes of elemental impurities based on "their toxicity (PDE) and likelihood of occurrence in the drug product" [47] (PDE = permitted daily exposure). Several elemental impurities in these classes are redox-active and/or catalyze oxidation reactions, such as Co, Ni and V (in class 2A); Ir, Os, Rh and Ru (in class 2B); and Cr, Cu and Mo (in class 3). The ICH Q3D(R2) guidelines list additional elemental impurities "for which PDE values have not been established due to their low inherent toxicity and/or differences in regional regulations" [47]. Of these, Fe, Mn and W are redox-active and/or catalyze oxidation reactions (as, perhaps, does Al [48]; here, $Al^{III}$ does not change its oxidation state but promotes the disproportionation reaction of two complexed $H_2O_2$ molecules). A representative quantitative analysis of the elemental impurities listed in class 1 and 2A in several formulation components predicts that their levels in

therapeutic protein drug products will be significantly below the PDE [49]. These elemental impurities will likely present no toxicological problems; however, even at levels below the PDE, some of these elemental impurities may promote radical formation and/or catalyze oxidation reactions. Therefore, we need to narrow down a selection of metals for further consideration in this article via other means. Class 2B elements "have a reduced probability of occurence in drug product" [47] and will, therefore, not be considered further. Lloyd et al. reported DNA oxidation in the presence of $H_2O_2$ for Cr(III), Fe(II), V(III) and Cu(II), indicating Fenton or Fenton-like reactivities of these metals [50]. However, no efficient DNA oxidation was observed for Co(II) and Ni(II) in the presence of $H_2O_2$ [50]. Anipsitakis and Dionysiou surveyed the formation of radicals from the reaction of three oxidants, including hydrogen peroxide ($H_2O_2$), potassium persulfate ($K_2S_2O_8$) and potassium peroxomono-sulfate ($KHSO_5$), with nine metals, including Fe(II), Fe(III), Co(II), Ru(III), Ag(I), Ce(III), V(III), Mn(II) and Ni(II) [51]. Of these, only Fe(II), Fe(III) and Ru(III) generated significant levels of hydroxyl radicals ($HO^\bullet$) upon reaction with $H_2O_2$ [51]. The other metals formed significant yields of inorganic radicals ($SO_4^{\bullet-}$) only upon reaction with $K_2S_2O_8$ and/or $KHSO_5$, oxidants that are likely not present in pharmaceutical formulations. In contrast, Stadtman et al. advocate for the formation of "caged" $HO^\bullet$ radicals during the reaction of Mn(II) with $H_2O_2$, available for the oxidation of substrates [52–54]. The data are consistent with respect to Co(II) and Ni(II), which we do not need to consider further as a source of radicals in pharmaceutical formulations. We will also not further consider any reactions of Mo(IV) as it functions as a co-catalyst in Fe-dependent Fenton reactions [55,56], for example, reducing Fe(III) to Fe(II) [55]. The formation and detection of $HO^\bullet$ radicals during reactions of V(III) and Mn(II) with $H_2O_2$ may depend on the experimental conditions; in a first approximation, the redox reactions of V(III) and Mn(II) with $H_2O_2$ would be rather comparable to the reactions of the Fe(II)/Fe(III) redox couple with $H_2O_2$. Hence, a more detailed description of the reaction mechanisms of Fe(II) and Fe(III) would serve as a model for analogous reactions of V(III) and Mn(II), and also of Cr(III) and Cu(II). Therefore, the following will entirely focus on processes of Fe-dependent radical generation through the Fenton reaction that are relevant to pharmaceutical formulations.

Reactions of Ferrous and Ferric Iron

In pharmaceutical formulations of therapeutic proteins, iron impurities can come from multiple sources, including the cell culture medium, manufacturing equipment, containers, proteins and excipients. Iron levels as high as 1–9 µM have been reported for some protein formulations [57,58].

In general, it can be assumed that iron impurities in pharmaceutical formulations will be present as ferric iron, $Fe^{III}$, coordinated with iron-binding ligands, L [59]. These ligands can originate from the protein as well as excipients such as amino acids and carbohydrates. Based on the formulation composition, it is likely that $Fe^{III}$ may be present in a variety of mixed ligand complexes, i.e., that complexes of $Fe^{III}$ show some heterogeneity. $Fe^{III}$ reacts with $H_2O_2$ according to equilibrium 3 [60,61].

$$L_xFe^{III} + H_2O_2 \rightleftharpoons L_xFe^{III}(^-O_2H) + H^+ \tag{3}$$
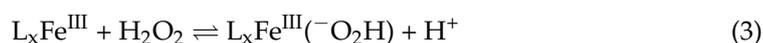
Rate constants of $k_3 = 69\,M^{-1}s^{-1}$ and $k_{-3} = 0.11\,s^{-1}$ have been reported for equilibrium 3 in acidic aqueous solution with pH 2.0 (where L = $H_2O$) [61]. Based on the standard reduction potentials for the couples $Fe^{III}/Fe^{II}$ (0.77 V vs. NHE) [62] and $HO_2/HO_2^-$ (0.79 V), the reduction of $Fe^{III}$ by $HO_2^-$ is feasible [63], so equilibrium 4 is reasonable, where the resulting hydroperoxyl radical is characterized by $pK_a$ = 4.8 for equilibrium 5 [64]. The superoxide radical anion ($O_2^{\bullet-}$) can subsequently reduce an additional equivalent of $L_xFe^{III}$ (reaction 6) [62,65].

$$L_xFe^{III}(^-O_2H) \rightleftharpoons L_xFe^{II} + HOO^\bullet \tag{4}$$

$$HOO^\bullet \rightleftharpoons H^+ + O_2^{\bullet-} \tag{5}$$

$$L_xFe^{III} + O_2^{\bullet-} \rightleftharpoons L_xFe^{II} + O_2 \tag{6}$$

However, it has been pointed out that, specifically, the reduction potential for the couple $Fe^{III}/Fe^{II}$ is very sensitive to pH [59] and the nature and concentration of the ligands [62,63], so the potential reduction of $L_xFe^{III}$ to $L_xFe^{II}$ by $HO_2^-$ must be carefully discussed with respect to these parameters. Specifically, for $L_x$ = EDTA, the reduction potential of $Fe^{III}/Fe^{II}$ decreases to 0.12 V [62], suggesting that the reduction of (EDTA)$Fe^{III}$ by $HO_2^-$ may not be a major pathway of $Fe^{II}$ formation [63] (for $L_x$ = DTPA, the reduction potential decreases even further to 0.03 V [66]). However, this prediction must be compared to experimental results that show that the reaction of $H_2O_2$ with (EDTA)$Fe^{III}$ yields an oxidant that converts the dipeptide Met-Met (Met = methionine) to products that are also generated via the exposure of Met-Met to a Fenton system, (EDTA)$Fe^{II}/H_2O_2$ [67], suggesting the formation of free or complexed hydroxyl radicals (HO$^\bullet$) or higher-valent iron-oxo species such as $Fe^{IV}$=O [61]. In this respect, the results of Bensaid et al. [42] are important, which show that the levels of iron impurities (20 ppb vs. <2 ppb) in formulations containing a monoclonal antibody, His, sucrose and polysorbate 80 control polysorbate oxidation, which correlates with the oxidation of Met[255] on the monoclonal antibody. In these formulations, it is likely that HO$^\bullet$ and/or $L_xFe^{IV}$=O are generated via the reaction of $L_xFe^{III}$ with hydrogen peroxide (reactions 3, 4, 7 and 8) and RO$^\bullet$ and/or $L_xFe^{IV}$=O via the reaction of $L_xFe^{II}$ with organic hydroperoxide impurities (reactions 10 and 11). Here, $L_xFe^{IV}$=O ($E^{o'}_{pH\,7.0} \approx 1.00$ V) is the less powerful and more selective oxidant compared to HO$^\bullet$ ($E^{o'}_{pH\,7.0} = 2.18$ V) [68].

$$L_xFe^{II} + H_2O_2 \rightarrow L_xFe^{III} + HO^\bullet + HO^- \tag{7}$$

$$L_xFe^{II} + H_2O_2 \rightarrow L_xFe^{IV}{=}O + H_2O \tag{8}$$

$$L_xFe^{III}(^-O_2R) \rightleftharpoons L_xFe^{II} + ROO^\bullet \tag{9}$$

$$L_xFe^{II} + HOOR \rightarrow L_xFe^{III} + RO^\bullet + HO^- \tag{10}$$

$$L_xFe^{II} + HOOR \rightarrow L_xFe^{IV}{=}O + ROH \tag{11}$$
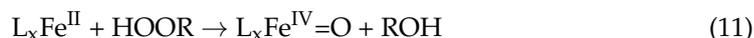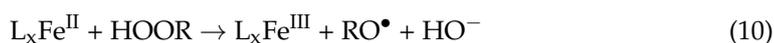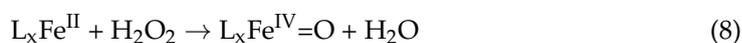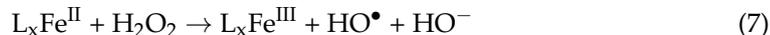
In this regard, the initial reaction (reaction 3) of $L_xFe^{III}$ with $H_2O_2$ may become important, as its product, $L_xFe^{III}(^-O_2H)$, reacts significantly more efficiently with $L_xFe^{II}$ ($k_{12} = 7.7 \times 10^5$ M$^{-1}$s$^{-1}$; L = $H_2O$, pH 1.0) compared to $H_2O_2$ ($k \approx 50$ M$^{-1}$s$^{-1}$) [61].

$$L_xFe^{III}(^-O_2H) + L_xFe^{II} \rightarrow L_xFe^{III} + [L_xFe^{III} + HO^\bullet]/L_xFe^{IV}{=}O \tag{12}$$

Ultimately, the resulting oxidizing species, HO$^\bullet$ and/or $L_xFe^{IV}$=O, will have the opportunity to react with formulation constituents such as protein and excipients, generating a plethora of oxidation products and secondary oxidizing species including peroxyl radicals, alkoxyl radicals and peroxides. The initial oxidation reactions of HO$^\bullet$ and/or $L_xFe^{IV}$=O may occur preferentially with the ligands L, coordinating either $Fe^{II}$ or $Fe^{III}$ [61]. Peroxyl and alkoxyl radicals, as well as peroxides, will be generated via the reaction of HO$^\bullet$ and/or $L_xFe^{IV}$=O with the organic constituents of the formulation. An alternative oxidant, the carbonate radical anion ($^\bullet CO_3^-$), may be generated if the formulation contains low amounts of bicarbonate (introduced through atmospheric $CO_2$), which can generate $L_xFe^{II}(CO_3)$ [69]. In such complexes, the initial oxidants, HO$^\bullet$ and/or $L_x(CO_3)Fe^{IV}$=O, may oxidize the Fe-bound carbonate to $^\bullet CO_3^-$ [69,70], which itself is a powerful yet more selective oxidant.

An important question is that of whether metal chelators can prevent the formation of oxidizing species during the reaction of peroxides with $L_xFe^{III}$ and $L_xFe^{II}$. Walling et al. [71] demonstrated the oxidation of a variety of organic substrates by $(EDTA)Fe^{III}/H_2O_2$, providing evidence that oxidation reactions prevail in the presence of EDTA. Likewise, Graf et al. showed that EDTA did not prevent the oxidation of dimethylsulfoxide (DMSO) (ultimately to formaldehyde) induced by $L_xFe^{III}$ and hypoxanthine/xanthine oxidase [72]. However, DTPA prevented the oxidation of DMSO, providing evidence that the chelator structure plays an important role in the efficiency of preventing substrate oxidation. These findings can, in part, be rationalized by the complex geometries of $(EDTA)Fe^{II}$ and $(EDTA)Fe^{III}$, where crystal structures demonstrate a distortion from octahedral geometry, resulting in the availability of a seventh binding site for a reaction to take place [73,74]. In aqueous solution, this seventh binding site generally coordinates with water [73,74], also indicated by a dissociable proton of $(EDTA)Fe^{III}(H_2O)$ with $pK_a \approx 7.6$ [75,76]. The bound water can be replaced by $H_2O_2$ [65,71,77] and, in case of $(EDTA)Fe^{II}$, also by molecular oxygen [78]. In fact, $(EDTA)Fe^{II}$ efficiently reacts with $H_2O_2$, with $k > 3 \times 10^3$ $M^{-1}s^{-1}$ [79,80].

### 3.3. Photochemical Generation of Radicals

Depending on the manufacturing environment and clinical use, protein formulations can be exposed to UVA and/or visible light [81], and an increasing number of studies show visible- or ambient-light-induced degradation of therapeutic proteins [58,82–92]. In particular, visible light photo-degradation is not easily rationalized with the known absorption characteristics of individual amino acids. This presents a challenge for the mechanistic analysis of processes leading to photo-degradation under visible light exposure, which is addressed in a recent review [93]. It is generally possible that photo-sensitizers are generated from the oxidative degradation of proteins and/or excipients, i.e., protein di-tyrosine from Tyr [94], 6a-hydroxy-2-oxo-octahydropyrollo[2,3-d]imidazole-5-carboxylic acid from His [17], advanced glycation end-products (AGEs) from the breakdown of carbohydrates [95], and cross-links between amino acids and lipid peroxidation products [96]. In addition, certain constituents or impurities present in cell culture media that co-purify with the protein may act as photo-sensitizers, e.g., riboflavin [97–99] or pterin derivatives [100–102]. These photo-sensitizers can generate radicals in pharmaceutical formulations via a type I process, which represents an electron transfer reaction by a photo-sensitizer, subsequent to which a radical intermediate reacts with oxygen [103] (in contrast, a type II process entails the generation of singlet oxygen, $^1O_2$ [103]).

Tryptophan residues can form cation-$\pi$ complexes [104–106], which absorb visible light [107,108]. In such complexes, the electron density is shared between the Trp $\pi$-system and the cation, resulting in spectroscopic properties reminiscent of $Trp^\bullet$ radicals [108]. Hence, Trp cation-$\pi$ complexes may serve as chromophores suitable for the initiation of photo-degradation by visible light, a possibility that should be tested experimentally.

In view of the discussion of $Fe^{III}$-dependent oxidation reactions in pharmaceutical formulations (see Section 3.2 above), the possibility of photo-Fenton reactions as a source of free radicals is a viable option. Pharmaceutical buffers (e.g., acetate, succinate, citrate) and amino acids contain carboxylate groups, where $Fe^{III}$-carboxylate complexes are characterized by broad absorption bands in the UVA and visible regions. Under light exposure, these $Fe^{III}$-carboxylate complexes can undergo ligand-to-metal-charge transfer (LMCT), reducing $Fe^{III}$ to $Fe^{II}$, and oxidizing the carboxylate ligand, which subsequently decarboxylates reactions (13) and (14) [109–113].

$$RCO_2^- \text{-}Fe^{III} \rightarrow RCO_2^\bullet \text{-}Fe^{II} \qquad (13)$$

$$RCO_2^\bullet \text{-}Fe^{II} \rightarrow R^\bullet + CO_2 + Fe^{II} \qquad (14)$$
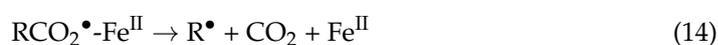
The resulting carbon-centered radical $R^\bullet$ will add oxygen to yield a peroxyl radical, $ROO^\bullet$, unless $R^\bullet$ is $^\bullet CO_2^-$ (see below), while $Fe^{II}$ reduces $O_2$ to $O_2^{\bullet-}$ [65] and $H_2O_2$ [114]. With respect to the necessary concentrations of $Fe^{III}$, basal levels of $Fe^{III}$ in 10 mM citrate

buffer, pH 6.0, were sufficient to promote the photo-oxidation of Met-enkephalin during near-UV photo-irradiation with a light dose of 25.2 Whm$^{-2}$ [115], i.e., ca. 1/8 of the light dose required according the ICH Q1B guidelines for photostability studies [116]. In these experiments, various lots of citrate were tested, and the photo-oxidation yields from Met-enkephalin correlated with the basal Fe$^{III}$ levels [115]. An important detail is the formation of $^{\bullet}CO_2^{-}$ during the photo-irradiation of citrate-Fe$^{III}$ with either near-UV or visible light, detected via spin-trapping with DMPO [115,117]. The $^{\bullet}CO_2^{-}$ radical is a powerful reductant (E$^{o}$(CO$_2$/$^{\bullet}$CO$_2^{-}$) $\approx 1.93 \pm 0.22$ V vs. NHE [118]) that reduces Fe$^{III}$ to Fe$^{II}$ [119], O$_2$ to O$_2^{\bullet-}$ [119,120] and disulfide (RSSR) to a thiyl radical (RS$^{\bullet}$) and thiolate (RS$^{-}$) [121–123].

Mechanistic studies suggest that the formation of $^{\bullet}CO_2^{-}$ from citrate involves LMCT from the (deprotonated) citrate hydroxyl group rather than the citrate carboxyl groups, generating an intermediary alkoxyl radical (RO$^{\bullet}$), which undergoes α-β cleavage of the central carboxylate group (Scheme 1; reactions 15 and 16) [117]. In reaction 15, the initial citrate-Fe$^{III}$ complex is drawn with reference to the crystal structure of mononuclear (citrate)$_2$Fe$^{III}$ [124], which shows that the hydroxyl group is deprotonated.
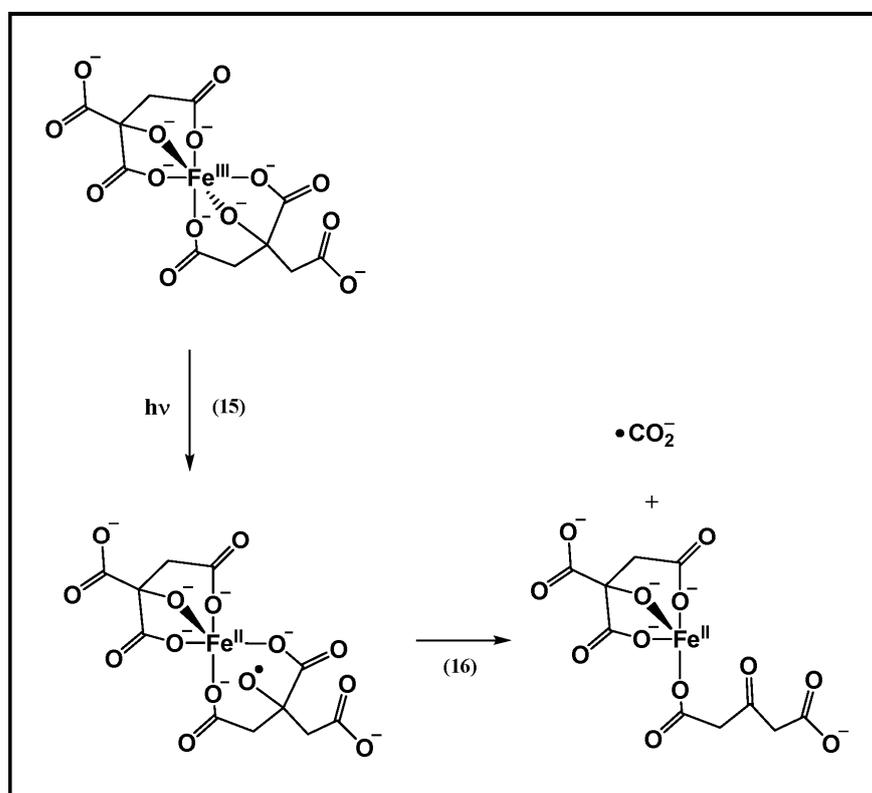


**Scheme 1.** Formation mechanism of $^{\bullet}CO_2^{-}$ from citrate-Fe$^{III}$ [117].

A similar mechanism was recently observed for a monoclonal antibody (IgG1) in the presence of Fe$^{III}$ and His buffer. In this case, photo-induced LMCT from a deprotonated Thr residue, Thr$^{259}$, led to an intermediary Thr side chain alkoxyl radical (Scheme 2, reaction 17), which underwent α-β cleavage, triggering side chain cleavage (Scheme 2, reaction 18) and, ultimately, backbone fragmentation [92].
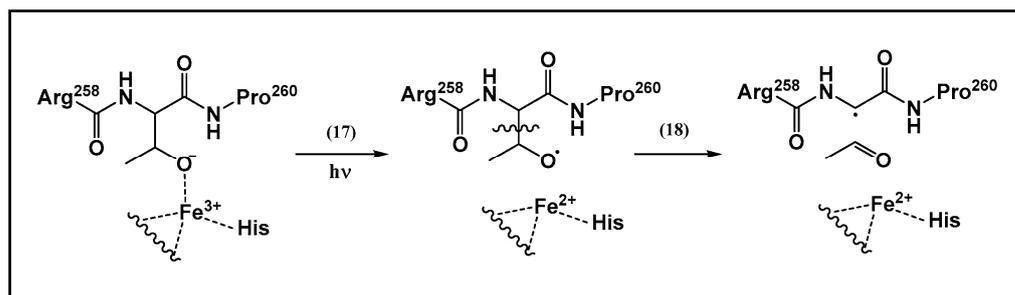
**Scheme 2.** LMCT mechanism leading to site-specific oxidation of a monoclonal antibody [92]. Photolytic generation of an alkoxyl radical at Thr[259] of IgG1 [92].

*3.4. Generation of Radicals via Mechanical Stress*

Protein formulations are exposed to various types of mechanical stress during manufacturing and transportation. Under certain circumstances, high shear stresses [125,126], mixing, pumping, filling [127–129] and mechanical shock [130–132] may lead to cavitation [133], a process that can cause the formation of HO$^\bullet$ radicals and even O atoms [134]. Hence, mechanical stresses have the potential to trigger the formation of highly oxidizing radicals, which can subsequently react with formulation constituents.

## 4. Protein Formulations Containing Additional Excipients

*4.1. Formulations Containing Antimicrobial Preservatives*

In order to ensure sterility, multidose formulations contain antimicrobial preservatives (APs) such as, e.g., phenol, m-cresol, benzyl alcohol, thimerosal or chlorobutanol [135,136] (for a summary of antimicrobial preservative-containing peptide and protein formulations listed in the *Physicians' Desk Reference*, PDR, see [135]). Some of the common antimicrobial preservatives are susceptible to oxidative degradation, potentially generating radicals in pharmaceutical formulations.

The exposure of benzyl alcohol to air leads to the slow formation of benzaldehyde, Ph-CHO [136]. Benzaldehyde spontaneously oxidizes to benzoic acid [137]. The latter pathway involves the formation of an intermediary benzoylperoxyl radical, Ph-C(O)OO$^\bullet$ (reactions 19 and 20), where In$^\bullet$ represents an initiating radical [137]. However, the presence of benzyl alcohol can suppress benzoic acid formation via the reaction of the benzoylperoxyl radical with benzylalcohol to generate peroxybenzoic acid, Ph-C(O)OOH, and an α-hydroxybenzyl radical, Ph-C$^\bullet$H-OH (reaction 21) [137]. The reaction of the α-hydroxybenzyl radical with molecular oxygen will ultimately generate benzaldehyde and superoxide (reaction 22).

$$\text{Ph-CHO} + \text{In}^\bullet \rightarrow \text{InH} + \text{Ph-}^\bullet\text{C(O)} \tag{19}$$

$$\text{Ph-}^\bullet\text{C(O)} + \text{O}_2 \rightarrow \text{Ph-C(O)OO}^\bullet \tag{20}$$

$$\text{Ph-C(O)OO}^\bullet + \text{Ph-CH}_2\text{OH} \rightarrow \text{Ph-C(O)OOH} + \text{Ph-C}^\bullet\text{H-OH} \tag{21}$$

$$\text{Ph-C}^\bullet\text{H-OH} + \text{O}_2 \rightarrow \text{Ph-CHO} + \text{H}^+/\text{O}_2^{\bullet-} \tag{22}$$

Therefore, formulations containing benzyl alcohol bear a potential risk for the formation of oxygen-centered radicals (peroxyl radicals, superoxide) and peroxides (peroxybenzoic acid).

The potential exposure of phenol and m-cresol to hydroxyl radicals (such as those generated by Fenton-type reactions; see Section 3.2 above) will lead to hydroxylation, preferentially in the ortho- or para-position with regard to the existing hydroxy substituent(s) [138–140]. Such hydroxylation reactions generate catechol derivatives, which can further promote Fenton-type reactions through redox cycling [141,142]. During redox cycling, a catechol derivative reduces $L_x\text{Fe}^{III}$ to $L_x\text{Fe}^{II}$, generating a semiquinone radical

(Scheme 3; equilibrium 23), which can further reduce $O_2$ to $O_2^{\bullet-}$ (equilibrium 24), generating a quinone derivative. The latter can comproportionate with a catechol to regenerate semiquinone derivatives (equilibrium 25) [142]. The dismutation of $O_2^{\bullet-}$ will generate $H_2O_2$, which will regenerate $L_xFe^{III}$ through a reaction with $L_xFe^{II}$, generating $HO^\bullet$ radicals (see Section 3.2).
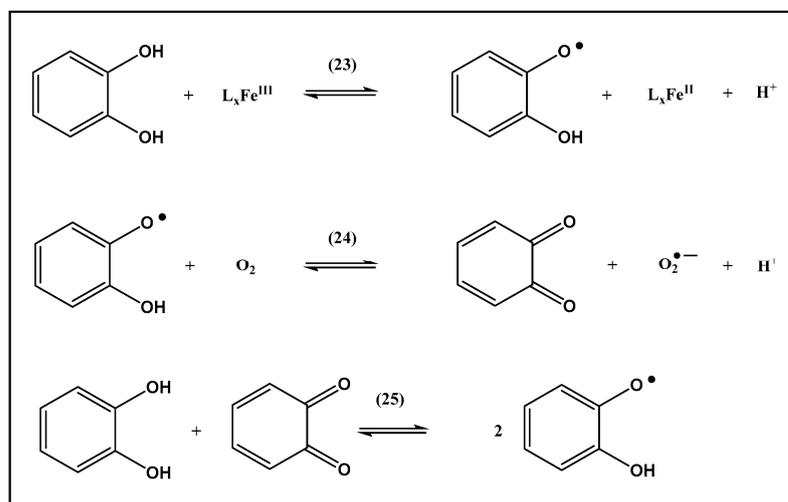


**Scheme 3.** Redox cycling of catechol.

### *4.2. Formulations Containing Zn(II)*

Specifically, insulin formulations, e.g., Humulin R® or Humalog®, contain Zn(II), generally in the form of ZnO (see package inserts for Humulin N® and Humalog®), which releases $Zn^{2+}$ [143]. ZnO confers antimicrobial activity [143], but the released $Zn^{2+}$ ions also support the formation of a native insulin hexamer [144]. Both Humulin N® and Humalog® also contain m-cresol and phenol, which are susceptible to hydroxylation and, subsequently, redox cycling (see Section 4.1). It was demonstrated that $Zn^{2+}$ increased total phenol oxidation (monitored as total organic carbon, TOC) during the Fenton oxidation of phenols, which has been rationalized by a more persistent semiquinone radical as a result of $Zn^{2+}$ complexation, generating more $HO^\bullet$ radicals [142]. Hence, the combination of phenols and $Zn^{2+}$ may increase the susceptibility of a formulation to Fenton oxidation.

An alternative mechanism by which ZnO, specifically, may promote oxidation reactions is photo-degradation. ZnO is a semiconductor with a band gap of 3.2–3.7 eV [145], which would require light with wavelengths of $\lambda$ = 387–335 nm to excite an electron from the valence band to the conduction band. Generally, the conduction band electron can reduce adsorbed $O_2$ to $O_2^{\bullet-}$, while the remaining positive hole, $h^+$, in the valence band can oxidize adsorbed $H_2O/HO^-$ to the $HO^\bullet$ radical [145,146]. ZnO was tested as a photocatalyst under light exposure with $\lambda$ > 300 nm on a coated glass plate [147], showing greater activity than $WO_3$, an activity comparable to that of brookite ($TiO_2$), but an activity lower than that of anatase ($TiO_2$). However, ZnO was more active than anatase in the photocatalytic degradation of humic acid in aqueous solution with pH 7.88 [148].

### 5. IV Enzyme Formulations for Enzyme Replacement Therapy

A review of IV formulations for enzyme replacement therapy [149,150] reveals that these formulations generally do not contain unusual excipients (for example, see package inserts for Aldurazyme®, Elaprase®, Vimizim®, Naglazyme®, Mepsevii®, VPRIV™ or Nexviazyme™). However, inspection of the active sites of the some of the relevant enzymes shows the presence of Cys residues, e.g., in N-acetylgalactosamine-6-sulfatase [151] and iduronate-2-sulfatase [152]. These Cys residues are post-translationally modified to $C_\alpha$-formylglycine (FGly) and, therefore, are not amenable to Cys oxidation.

## 6. Conclusions

Based on information on impurities and stress factors that affect pharmaceutical formulations, a series of mechanisms are formulated that could be responsible for free radical formation in pharmaceutical formulations. The focus of this article is on highly probable reactions; additional pathways may be possible in isolated cases when pharmaceutical formulations contain high levels of specific impurities that are not generally present. With respect to the design of stress tests for pharmaceutical formulations, highly probable reactions should be kept in mind. For example, it may be questionable whether the addition of $Fe^{II}$ to a pharmaceutical formulation may generate information about the kinetics of iron-dependent oxidation degradation reactions under storage conditions, as iron impurities will likely be present as $Fe^{III}$. However, the addition of $Fe^{II}$ may lead to mechanistic information that can be used to predict certain degradation pathways in cases whereby $Fe^{III}$ is converted to $Fe^{II}$, for example, through reaction with $H_2O_2$ or hydroperoxides. A limitation of mechanistic investigations of radical-induced oxidation reactions in pharmaceutical formulations will always be that the precise quantity and nature of the radicals specifically generated under storage conditions are usually unknown. Even the monounsaturated oleic acid, the main component of polysorbate 80 fatty acid esters [35,36], can generate a number of different peroxyl radicals [40]. It is unknown to what extent the nature of these different peroxyl radicals would affect the kinetics of chain propagation within polysorbate 80 micelles. This question may be addressed through the quantification of specific reaction products that are representative of individual oxidation pathways, a task that may require the modification or improvement of analytical methodology, potentially supported by artificial intelligence.

**Conflicts of Interest:** The author declares no conflict of interest.

## References

1. Strickley, R.G.; Lambert, W.J. A review of Formulations of Commercially Available Antibodies. *J. Pharm. Sci.* **2021**, *110*, 2590–2608. [CrossRef]
2. Manning, M.C.; Chou, D.K.; Murphy, B.M.; Payne, R.W.; Katayama, D.S. Stability of protein pharmaceuticals: An update. *Pharm. Res.* **2010**, *27*, 544–575. [CrossRef] [PubMed]
3. Manning, M.C.; Liu, J.; Li, T.; Holcomb, R.E. Rational Design of Liquid Formulations of Proteins. *Adv. Protein Chem. Struct. Biol.* **2018**, *112*, 1–59. [PubMed]
4. Wang, W.; Ohtake, S. Science and art of protein formulation development. *Int. J. Pharm.* **2019**, *568*, 118505. [CrossRef] [PubMed]
5. Falconer, R.J. Advances in liquid formulations of parenteral therapeutic proteins. *Biotechnol. Adv.* **2019**, *37*, 107412. [CrossRef]
6. Gupta, S.; Jiskoot, W.; Schöneich, C.; Rathore, A.S. Oxidation and Deamidation of Monoclonal Antibody Products: Potential Impact on Stability, Biological Activity, and Efficacy. *J. Pharm. Sci.* **2022**, *111*, 903–918. [CrossRef] [PubMed]
7. Jiskoot, W.; Hawe, A.; Menzen, T.; Volkin, D.B.; Crommelin, D.J.A. Ongoing Challenges to Develop High Concentration Monoclonal Antibody-based Formulations for Subcutaneous Administration: Quo Vadis? *J. Pharm. Sci.* **2022**, *111*, 861–867. [CrossRef] [PubMed]
8. Hawkins, C.L.; Davies, M.J. Detection, identification, and quantification of oxidative protein modifications. *J. Biol. Chem.* **2019**, *294*, 19683–19708. [CrossRef]
9. Fuentes-Lemus, E.; Hagglund, P.; Lopez-Alarcon, C.; Davies, M.J. Oxidative Crosslinking of Peptides and Proteins: Mechanisms of Formation, Detection, Characterization and Quantification. *Molecules* **2021**, *27*, 15. [CrossRef]
10. Ho, E.; Karimi Galougahi, K.; Liu, C.C.; Bhindi, R.; Figtree, G.A. Biological markers of oxidative stress: Applications to cardiovascular research and practice. *Redox Biol.* **2013**, *1*, 483–491. [CrossRef]
11. Tucker, P.S.; Dalbo, V.J.; Han, T.; Kingsley, M.I. Clinical and research markers of oxidative stress in chronic kidney disease. *Biomarkers* **2013**, *18*, 103–115. [CrossRef] [PubMed]
12. Cristani, M.; Speciale, A.; Saija, A.; Gangemi, S.; Minciullo, P.L.; Cimino, F. Circulating Advanced Oxidation Protein Products as Oxidative Stress Biomarkers and Progression Mediators in Pathological Conditions Related to Inflammation and Immune Dysregulation. *Curr. Med. Chem.* **2016**, *23*, 3862–3882. [CrossRef] [PubMed]

13. Kadiiska, M.B.; Gladen, B.C.; Baird, D.D.; Germolec, D.; Graham, L.B.; Parker, C.E.; Nyska, A.; Wachsman, J.T.; Ames, B.N.; Basu, S.; et al. Biomarkers of oxidative stress study II: Are oxidation products of lipids, proteins, and DNA markers of CCl4 poisoning? *Free Radic. Biol. Med.* **2005**, *38*, 698–710. [CrossRef] [PubMed]

14. Kadiiska, M.B.; Basu, S.; Brot, N.; Cooper, C.; Saari Csallany, A.; Davies, M.J.; George, M.M.; Murray, D.M.; Jackson Roberts, L., 2nd; Shigenaga, M.K.; et al. Biomarkers of oxidative stress study V: Ozone exposure of rats and its effect on lipids, proteins, and DNA in plasma and urine. *Free Radic. Biol. Med.* **2013**, *61*, 408–415. [CrossRef] [PubMed]

15. Hipper, E.; Blech, M.; Hinderberger, D.; Garidel, P.; Kaiser, W. Photo-Oxidation of Therapeutic Protein Formulations: From Radical Formation to Analytical Techniques. *Pharmaceutics* **2022**, *14*, 72. [CrossRef]

16. Mason, B.D.; McCracken, M.; Bures, E.J.; Kerwin, B.A. Oxidation of free L-histidine by tert-Butylhydroperoxide. *Pharm. Res.* **2010**, *27*, 447–456. [CrossRef] [PubMed]

17. Stroop, S.D.; Conca, D.M.; Lundgard, R.P.; Renz, M.E.; Peabody, L.M.; Leigh, S.D. Photosensitizers form in histidine buffer and mediate the photodegradation of a monoclonal antibody. *J. Pharm. Sci.* **2011**, *100*, 5142–5155. [CrossRef] [PubMed]

18. Wang, T.; Markham, A.; Thomas, S.J.; Wang, N.; Huang, L.; Clemens, M.; Rajagopalan, N. Solution Stability of Poloxamer 188 Under Stress Conditions. *J. Pharm. Sci.* **2019**, *108*, 1264–1271. [CrossRef]

19. Zheng, X.W.; Sutton, A.T.; Yang, R.S.; Miller, D.V.; Pagels, B.; Rustandi, R.R.; Welch, J.; Payne, A.; Haverick, M. Extensive Characterization of Polysorbate 80 Oxidative Degradation Under Stainless Steel Conditions. *J. Pharm. Sci.* **2023**, *112*, 779–789. [CrossRef] [PubMed]

20. Kishore, R.S.; Kiese, S.; Fischer, S.; Pappenberger, A.; Grauschopf, U.; Mahler, H.C. The degradation of polysorbates 20 and 80 and its potential impact on the stability of biotherapeutics. *Pharm. Res.* **2011**, *28*, 1194–1210. [CrossRef] [PubMed]

21. Kishore, R.S.; Pappenberger, A.; Dauphin, I.B.; Ross, A.; Buergi, B.; Staempfli, A.; Mahler, H.C. Degradation of polysorbates 20 and 80: Studies on thermal autoxidation and hydrolysis. *J. Pharm. Sci.* **2011**, *100*, 721–731. [CrossRef] [PubMed]

22. Borisov, O.V.; Ji, J.A.; Wang, Y.J.; Vega, F.; Ling, V.T. Toward understanding molecular heterogeneity of polysorbates by application of liquid chromatography-mass spectrometry with computer-aided data analysis. *Anal. Chem.* **2011**, *83*, 3934–3942. [CrossRef] [PubMed]

23. Borisov, O.V.; Ji, J.A.; John Wang, Y. Oxidative Degradation of Polysorbate Surfactants Studied by Liquid Chromatography-Mass Spectrometry. *J. Pharm. Sci.* **2015**, *104*, 1005–1018. [CrossRef]

24. Kranz, W.; Wuchner, K.; Corradini, E.; Menzen, T.; Hawe, A. Micelle Driven Oxidation Mechansim and Novel Oxidation Markers for Different Grades of Polysorbate 20 and 80. *J. Pharm. Sci.* **2020**, *109*, 3064–3077. [CrossRef] [PubMed]

25. Hille, R. Xanthine Oxidase-A Personal History. *Molecules* **2023**, *28*, 1921. [CrossRef] [PubMed]

26. Stuehr, D.J.; Haque, M.M. Nitric oxide synthase enzymology in the 20 years after the Nobel Prize. *Br. J. Pharmacol.* **2019**, *176*, 177–188. [CrossRef]

27. Hawkins, C.L.; Davies, M.J. Role of myeloperoxidase and oxidant formation in the extracellular environment in inflammation-induced tissue damage. *Free Radic. Biol. Med.* **2021**, *172*, 633–651. [CrossRef]

28. Schröder, K. NADPH oxidases: Current aspects and tools. *Redox Biol.* **2020**, *34*, 101512. [CrossRef]

29. Mieczkowski, C.A. The Evolution of Commercial Antibody Formulations. *J. Pharm. Sci.* **2023**, *112*, 1801–1810. [CrossRef]

30. Miller, D.M.; Buettner, G.R.; Aust, S.D. Transition metals as catalysts of "autoxidation" reactions. *Free Radic. Biol. Med.* **1990**, *8*, 95–108. [CrossRef]

31. Merenyi, G.; Lind, J.; Jonsson, M. Autoxidation of Closed-Shell Organics—An Outer-Sphere Electron-Transfer. *J. Am. Chem. Soc.* **1993**, *115*, 4945–4946. [CrossRef]

32. Prutz, W.A.; Butler, J.; Land, E.J.; Swallow, A.J. Unpaired electron migration between aromatic and sulfur peptide units. *Free Radic. Res. Commun.* **1986**, *2*, 69–75. [CrossRef] [PubMed]

33. Surdhar, P.S.; Armstrong, D.A. Reduction Potentials and Exchange-Reactions of Thiyl Radicals and Disulfide Anion Radicals. *J. Phys. Chem.* **1987**, *91*, 6532–6537. [CrossRef]

34. Howard, J.A. Homogenous Liquid-Phase Autoxidations. In *Free Radicals*; Kochi, J.K., Ed.; Wiley: New York, NY, USA, 1973; Volume 2, pp. 3–62.

35. Dwivedi, M.; Blech, M.; Presser, I.; Garidel, P. Polysorbate degradation in biotherapeutic formulations: Identification and discussion of current root causes. *Int. J. Pharm.* **2018**, *552*, 422–436. [CrossRef]

36. Konya, Y.; Ochiai, R.; Fujiwara, S.; Tsujino, K.; Okumura, T. Profiling polysorbate 80 components using comprehensive liquid chromatography-tandem mass spectrometry analysis. *Rapid Commun. Mass Spectrom.* **2023**, *37*, e9438. [CrossRef]

37. Mittag, J.J.; Trutschel, M.L.; Kruschwitz, H.; Mader, K.; Buske, J.; Garidel, P. Characterization of radicals in polysorbate 80 using electron paramagnetic resonance (EPR) spectroscopy and spin trapping. *Int. J. Pharm. X* **2022**, *4*, 100123. [CrossRef]

38. Ha, E.; Wang, W.; Wang, Y.J. Peroxide formation in polysorbate 80 and protein stability. *J. Pharm. Sci.* **2002**, *91*, 2252–2264. [CrossRef]

39. Morita, M.; Tokita, M. The real radical generator other than main-product hydroperoxide in lipid autoxidation. *Lipids* **2006**, *41*, 91–95. [CrossRef]

40. Porter, N.A. A Perspective on Free Radical Autoxidation: The Physical Organic Chemistry of Polyunsaturated Fatty Acid and Sterol Peroxidation. *J. Org. Chem.* **2013**, *78*, 3511–3524. [CrossRef]

41. Mayo, F.R.; Miller, A.A. Oxidation of Unsaturated Compounds. 2. Reactions of Styrene Peroxide. *J. Am. Chem. Soc.* **1956**, *78*, 1023–1034. [CrossRef]

42. Bensaid, F.; Dagallier, C.; Authelin, J.R.; Audat, H.; Filipe, V.; Narradon, C.; Guibal, P.; Clavier, S.; Wils, P. Mechanistic understanding of metal-catalyzed oxidation of polysorbate 80 and monoclonal antibody in biotherapeutic formulations. *Int. J. Pharm.* **2022**, *615*, 121496. [CrossRef] [PubMed]

43. Gopalrathnam, G.; Sharma, A.N.; Dodd, S.W.; Huang, L. Impact of Stainless Steel Exposure on the Oxidation of Polysorbate 80 in Histidine Placebo and Active Monoclonal Antibody Formulation. *PDA J. Pharm. Sci. Technol.* **2018**, *72*, 163–175. [CrossRef]

44. Wasylaschuk, W.R.; Harmon, P.A.; Wagner, G.; Harman, A.B.; Templeton, A.C.; Xu, H.; Reed, R.A. Evaluation of hydroperoxides in common pharmaceutical excipients. *J. Pharm. Sci.* **2007**, *96*, 106–116. [CrossRef]

45. Ding, S. Quantitation of hydroperoxides in the aqueous solutions of non-ionic surfactants using polysorbate 80 as the model surfactant. *J. Pharm. Biomed. Anal.* **1993**, *11*, 95–101. [CrossRef] [PubMed]

46. Noh, M.S.; Jung, S.H.; Kwon, O.; Lee, S.I.; Yang, S.J.; Hahm, E.; Jun, B.H. Evaluation of Sterilization Performance for Vaporized-Hydrogen-Peroxide-Based Sterilizer with Diverse Controlled Parameters. *ACS Omega* **2020**, *5*, 29382–29387. [CrossRef]

47. *Q3D(R2) Elemental Impurities. Guidance for Industry*; International Council for Harmonization (ICH): Geneva, Switzerland, 2022.

48. Kuznetsov, M.L.; Kozlov, Y.N.; Mandelli, D.; Pombeiro, A.J.L.; Shul'pin, G.B. Mechanism of Al$^{3+}$-Catalyzed Oxidations of Hydrocarbons: Dramatic Activation of H$_2$O$_2$ toward O-O Homolysis in Complex [Al(H$_2$O)$_4$(OOH)(H$_2$O$_2$)]$^{2+}$ Explains the Formation of HO center dot Radicals. *Inorg. Chem.* **2011**, *50*, 3996–4005. [CrossRef] [PubMed]

49. Luo, Y.; Sekhar, C.; Lee, H.; Fujimori, K.; Ronk, M.; Semin, D.; Nashed-Samuel, Y. A Risk-Based Approach to Evaluate and Control Elemental Impurities in Therapeutic Proteins. *J. Pharm. Sci.* **2020**, *109*, 3378–3385. [CrossRef]

50. Lloyd, D.R.; Carmichael, P.L.; Phillips, D.H. Comparison of the formation of 8-hydroxy-2'-deoxyguanosine and single- and double-strand breaks in DNA mediated by fenton reactions. *Chem. Res. Toxicol.* **1998**, *11*, 420–427. [CrossRef]

51. Anipsitakis, G.P.; Dionysiou, D.D. Radical generation by the interaction of transition metals with common oxidants. *Environ. Sci. Technol.* **2004**, *38*, 3705–3712. [CrossRef]

52. Stadtman, E.R.; Berlett, B.S.; Chock, P.B. Manganese-dependent disproportionation of hydrogen peroxide in bicarbonate buffer. *Proc. Natl. Acad. Sci. USA* **1990**, *87*, 384–388. [CrossRef]

53. Berlett, B.S.; Chock, P.B.; Yim, M.B.; Stadtman, E.R. Manganese(II) catalyzes the bicarbonate-dependent oxidation of amino acids by hydrogen peroxide and the amino acid-facilitated dismutation of hydrogen peroxide. *Proc. Natl. Acad. Sci. USA* **1990**, *87*, 389–393. [CrossRef] [PubMed]

54. Yim, M.B.; Berlett, B.S.; Chock, P.B.; Stadtman, E.R. Manganese(II)-bicarbonate-mediated catalytic activity for hydrogen peroxide dismutation and amino acid oxidation: Detection of free radical intermediates. *Proc. Natl. Acad. Sci. USA* **1990**, *87*, 394–398. [CrossRef]

55. Liu, J.; Dong, C.C.; Deng, Y.X.; Ji, J.H.; Bao, S.Y.; Chen, C.R.; Shen, B.; Zhang, J.L.; Xing, M.Y. Molybdenum sulfide Co-catalytic Fenton reaction for rapid and efficient inactivation of Escherichia colis. *Water Res.* **2018**, *145*, 312–320. [CrossRef]

56. Yang, J.C.; Yao, H.L.; Guo, Y.D.; Yang, B.W.; Shi, J.L. Enhancing Tumor Catalytic Therapy by Co-Catalysis. *Angew. Chem. Int. Ed.* **2022**, *61*, e202200480.

57. Ouellette, D.; Alessandri, L.; Piparia, R.; Aikhoje, A.; Chin, A.; Radziejewski, C.; Correia, I. Elevated cleavage of human immunoglobulin gamma molecules containing a lambda light chain mediated by iron and histidine. *Anal. Biochem.* **2009**, *389*, 107–117. [CrossRef] [PubMed]

58. Adem, Y.T.; Molina, P.; Liu, H.; Patapoff, T.W.; Sreedhara, A.; Esue, O. Hexyl glucoside and hexyl maltoside inhibit light-induced oxidation of tryptophan. *J. Pharm. Sci.* **2014**, *103*, 409–416. [CrossRef]

59. Koppenol, W.H.; Hider, R.H. Iron and redox cycling. Do's and don'ts. *Free Radic. Biol. Med.* **2019**, *133*, 3–10. [CrossRef]

60. Rachmilovich-Calis, S.; Masarwa, A.; Meyerstein, N.; Meyerstein, D.; van Eldik, R. New Mechanistic Aspects of the Fenton Reaction. *Chem.-Eur. J.* **2009**, *15*, 8303–8309. [CrossRef]

61. Meyerstein, D. What Are the Oxidizing Intermediates in the Fenton and Fenton-like Reactions? A Perspective. *Antioxidants* **2022**, *11*, 1368. [CrossRef]

62. Pierre, J.L.; Fontecave, M.; Crichton, R.R. Chemistry for an essential biological process: The reduction of ferric iron. *Biometals* **2002**, *15*, 341–346. [CrossRef]

63. Chen, H.Y.; Lin, Y.F. DFT study on the catalytic decomposition of hydrogen peroxide by iron complexes of nitrilotriacetate. *J. Comput. Chem.* **2023**. [CrossRef] [PubMed]

64. Bielski, B.H.; Cabelli, D.E. Highlights of current research involving superoxide and perhydroxyl radicals in aqueous solutions. *Int. J. Radiat. Biol.* **1991**, *59*, 291–319. [CrossRef] [PubMed]

65. Bull, C.; McClune, G.J.; Fee, J.A. The Mechanism of Fe-Edta Catalyzed Superoxide Dismutation. *J. Am. Chem. Soc.* **1983**, *105*, 5290–5300. [CrossRef]

66. Vandegaer, J.; Chaberek, S.; Frost, A.E. Iron Chelates of Diethylenetriaminepentaacetic Acid. *J. Inorg. Nucl. Chem.* **1959**, *11*, 210–221. [CrossRef]

67. Hong, J.; Schöneich, C. The metal-catalyzed oxidation of methionine in peptides by Fenton systems involves two consecutive one-electron oxidation processes. *Free Radic. Biol. Med.* **2001**, *31*, 1432–1441. [CrossRef]

68. Koppenol, W.H.; Liebman, J.F. The Oxidizing Nature of the Hydroxyl Radical—A Comparison with the Ferryl Ion (Feo2+). *J. Phys. Chem.* **1984**, *88*, 99–101. [CrossRef]

69. Illes, E.; Mizrahi, A.; Marks, V.; Meyerstein, D. Carbonate-radical-anions, and not hydroxyl radicals, are the products of the Fenton reaction in neutral solutions containing bicarbonate. *Free Radic. Biol. Med.* **2019**, *131*, 1–6. [CrossRef]

70. Patra, S.G.; Mizrahi, A.; Meyerstein, D. The Role of Carbonate in Catalytic Oxidations. *Accounts Chem. Res.* **2020**, *53*, 2189–2200. [CrossRef]

71. Walling, C.; Kurz, M.; Schugar, H.J. Iron(III)-Ethylenediaminetetraacetic Acid-Peroxide System. *Inorg. Chem.* **1970**, *9*, 931. [CrossRef]

72. Graf, E.; Mahoney, J.R.; Bryant, R.G.; Eaton, J.W. Iron-catalyzed hydroxyl radical formation. Stringent requirement for free iron coordination site. *J. Biol. Chem.* **1984**, *259*, 3620–3624. [CrossRef]

73. Lind, M.D.; Hoard, J.L.; Hamor, M.J.; Hamor, T.A. Stereocnemistry of ethylenediaminetetraacetato complexes. II. The structure of crystalline $Rb[Fe(OH_2)Y].H_2O^{1-3}$. III. The structure of crystalline $Li[Fe(OH_2Y].2H_2O^{1-3}$. *Inorg. Chem.* **1964**, *3*, 34. [CrossRef]

74. Mizuta, T.; Wang, J.; Miyoshi, K. Molecular-Structures of Fe(II) Complexes with Monoprotonated and Diprotonated Ethylenediamine-N,N,N',N'-Tetraacetate (Hedta and H2edta), as Determined by X-Ray Crystal Analyses. *Inorg. Chim. Acta* **1995**, *230*, 119–125. [CrossRef]

75. Schwarzenbach, G.; Heller, J. Komplexone. 18. Die Eisen(II) Und Eisen(III)-Komplexe Der Athylendiamin-Tetraessigsaure Und Ihr Redoxgleichgewicht. *Helv. Chim. Acta* **1951**, *34*, 576–591. [CrossRef]

76. Gustafson, R.L.; Martell, A.E. Hydrolytic Tendencies of Ferric Chelates. *J. Phys. Chem.* **1963**, *67*, 576–582. [CrossRef]

77. Brausam, A.; van Eldik, R. Further mechanistic information on the reaction between Fe-III(edta) and hydrogen peroxide: Observation of a second reaction step and importance of pH. *Inorg. Chem.* **2004**, *43*, 5351–5359. [CrossRef]

78. Seibig, S.; vanEldik, R. Kinetics of [Fe-II(edta)] oxidation by molecular oxygen revisited. New evidence for a multistep mechanism. *Inorg. Chem.* **1997**, *36*, 4115–4120. [CrossRef]

79. Rush, J.D.; Koppenol, W.H. Oxidizing intermediates in the reaction of ferrous EDTA with hydrogen peroxide. Reactions with organic molecules and ferrocytochrome c. *J. Biol. Chem.* **1986**, *261*, 6730–6733. [CrossRef]

80. Rush, J.D.; Koppenol, W.H. The reaction between ferrous polyaminocarboxylate complexes and hydrogen peroxide: An investigation of the reaction intermediates by stopped flow spectrophotometry. *J. Inorg. Biochem.* **1987**, *29*, 199–215. [CrossRef]

81. Baertschi, S.W.; Clapham, D.; Foti, C.; Jansen, P.J.; Kristensen, S.; Reed, R.A.; Templeton, A.C.; Tonnesen, H.H. Implications of in-use photostability: Proposed guidance for photostability testing and labeling to support the administration of photosensitive pharmaceutical products, part 1: Drug products administered by injection. *J. Pharm. Sci.* **2013**, *102*, 3888–3899. [CrossRef]

82. Kerwin, B.A.; Remmele, R.L. Protect from light: Photodegradation and protein biologics. *J. Pharm. Sci.* **2007**, *96*, 1468–1479. [CrossRef]

83. Mallaney, M.; Wang, S.H.; Sreedhara, A. Effect of ambient light on monoclonal antibody product quality during small-scale mammalian cell culture process in clear glass bioreactors. *Biotechnol. Prog.* **2014**, *30*, 562–570. [CrossRef]

84. Sreedhara, A.; Yin, J.; Joyce, M.; Lau, K.; Wecksler, A.T.; Deperalta, G.; Yi, L.; John Wang, Y.; Kabakoff, B.; Kishore, R.S. Effect of ambient light on IgG1 monoclonal antibodies during drug product processing and development. *Eur. J. Pharm. Biopharm.* **2016**, *100*, 38–46. [CrossRef]

85. Luis, L.M.; Hu, Y.; Zamiri, C.; Sreedhara, A. Determination of the Acceptable Ambient Light Exposure during Drug Product Manufacturing for Long-Term Stability of Monoclonal Antibodies. *PDA J. Pharm. Sci. Technol.* **2018**, *72*, 393–403. [CrossRef]

86. Liu, M.; Zhang, Z.; Cheetham, J.; Ren, D.; Zhou, Z.S. Discovery and characterization of a photo-oxidative histidine-histidine cross-link in IgG1 antibody utilizing (1)(8)O-labeling and mass spectrometry. *Anal. Chem.* **2014**, *86*, 4940–4948. [CrossRef]

87. Lei, M.; Carcelen, T.; Walters, B.T.; Zamiri, C.; Quan, C.; Hu, Y.; Nishihara, J.; Yip, H.; Woon, N.; Zhang, T.; et al. Structure-Based Correlation of Light-Induced Histidine Reactivity in A Model Protein. *Anal. Chem.* **2017**, *89*, 7225–7231. [CrossRef]

88. Lei, M.; Quan, C.; Wang, Y.J.; Kao, Y.H.; Schöneich, C. Light-Induced Covalent Buffer Adducts to Histidine in a Model Protein. *Pharm. Res.* **2018**, *35*, 67. [CrossRef]

89. Bane, J.; Mozziconacci, O.; Yi, L.; Wang, Y.J.; Sreedhara, A.; Schöneich, C. Photo-oxidation of IgG1 and Model Peptides: Detection and Analysis of Triply Oxidized His and Trp Side Chain Cleavage Products. *Pharm. Res.* **2017**, *34*, 229–242. [CrossRef]

90. Kaiser, W.; Schultz-Fademrecht, T.; Blech, M.; Buske, J.; Garidel, P. Investigating photodegradation of antibodies governed by the light dosage. *Int. J. Pharm.* **2021**, *604*, 120723. [CrossRef]

91. More, H.T.; Bindra, D.S.; Zumba, A.; Zhou, K.; Carvalho, T.; Mantri, R. Effect of light source and UVA quotient on monoclonal antibody stability during ambient light exposure studies. *Eur. J. Pharm. Biopharm.* **2023**, *185*, 177–182. [CrossRef]

92. Zhang, Y.; Schöneich, C. Visible Light Induces Site-Specific Oxidative Heavy Chain Fragmentation of a Monoclonal Antibody (IgG1) Mediated by an Iron(III)-Containing Histidine Buffer. *Mol. Pharm.* **2023**, *20*, 650–662. [CrossRef]

93. Schöneich, C. Photo-Degradation of Therapeutic Proteins: Mechanistic Aspects. *Pharm. Res.* **2020**, *37*, 45. [CrossRef] [PubMed]

94. Reid, L.O.; Vignoni, M.; Martins-Froment, N.; Thomas, A.H.; Dantola, M.L. Photochemistry of tyrosine dimer: When an oxidative lesion of proteins is able to photoinduce further damage. *Photochem. Photobiol. Sci.* **2019**, *18*, 1732–1741. [CrossRef] [PubMed]

95. Masaki, H.; Okano, Y.; Sakurai, H. Generation of active oxygen species from advanced glycation end-products (AGEs) during ultraviolet light A (UVA) irradiation and a possible mechanism for cell damaging. *Biochim. Biophys. Acta* **1999**, *1428*, 45–56. [CrossRef]

96. Lamore, S.D.; Azimian, S.; Horn, D.; Anglin, B.L.; Uchida, K.; Cabello, C.M.; Wondrak, G.T. The malondialdehyde-derived fluorophore DHP-lysine is a potent sensitizer of UVA-induced photooxidative stress in human skin cells. *J. Photochem. Photobiol. B* **2010**, *101*, 251–264. [CrossRef] [PubMed]

97. Karran, P.; Brem, R. Protein oxidation, UVA and human DNA repair. *DNA Repair* **2016**, *44*, 178–185. [CrossRef] [PubMed]

98. Cardoso, D.R.; Franco, D.W.; Olsen, K.; Andersen, M.L.; Skibsted, L.H. Reactivity of bovine whey proteins, peptides, and amino acids toward triplet riboflavin as studied by laser flash photolysis. *J. Agric. Food Chem.* **2004**, *52*, 6602–6606. [CrossRef]

99. Huvaere, K.; Skibsted, L.H. Light-induced oxidation of tryptophan and histidine. Reactivity of aromatic N-heterocycles toward triplet-excited flavins. *J. Am. Chem. Soc.* **2009**, *131*, 8049–8060. [CrossRef] [PubMed]

100. Castano, C.; Dantola, M.L.; Oliveros, E.; Thomas, A.H.; Lorente, C. Oxidation of tyrosine photoinduced by pterin in aqueous solution. *Photochem. Photobiol.* **2013**, *89*, 1448–1455. [CrossRef]

101. Thomas, A.H.; Lorente, C.; Roitman, K.; Morales, M.M.; Dantola, M.L. Photosensitization of bovine serum albumin by pterin: A mechanistic study. *J. Photochem. Photobiol. B* **2013**, *120*, 52–58. [CrossRef]

102. Reid, L.O.; Dantola, M.L.; Petroselli, G.; Erra-Balsells, R.; Miranda, M.A.; Lhiaubet-Vallet, V.; Thomas, A.H. Chemical Modifications of Globular Proteins Phototriggered by an Endogenous Photosensitizer. *Chem. Res. Toxicol.* **2019**, *32*, 2250–2259. [CrossRef]

103. Baptista, M.S.; Cadet, J.; Di Mascio, P.; Ghogare, A.A.; Greer, A.; Hamblin, M.R.; Lorente, C.; Nunez, S.C.; Ribeiro, M.S.; Thomas, A.H.; et al. Type I and Type II Photosensitized Oxidation Reactions: Guidelines and Mechanistic Pathways. *Photochem. Photobiol.* **2017**, *93*, 912–919. [CrossRef]

104. Dougherty, D.A. Cation-pi interactions in chemistry and biology: A new view of benzene, Phe, Tyr, and Trp. *Science* **1996**, *271*, 163–168. [CrossRef] [PubMed]

105. Gallivan, J.P.; Dougherty, D.A. Cation-pi interactions in structural biology. *Proc. Natl. Acad. Sci. USA* **1999**, *96*, 9459–9464. [CrossRef]

106. Dougherty, D.A. The cation-pi interaction. *Acc. Chem. Res.* **2013**, *46*, 885–893. [CrossRef] [PubMed]

107. Roveri, O.A.; Braslavsky, S.E. pi-Cation interactions as the origin of the weak absorption at 532 nm observed in tryptophan-containing polypeptides. *Photochem. Photobiol. Sci.* **2012**, *11*, 962–966. [CrossRef] [PubMed]

108. Juszczak, L.J.; Eisenberg, A.S. The Color of Cation-pi Interactions: Subtleties of Amine-Tryptophan Interaction Energetics Allow for Radical-like Visible Absorbance and Fluorescence. *J. Am. Chem. Soc.* **2017**, *139*, 8302–8311. [CrossRef]

109. Chen, J.; Browne, W.R. Photochemistry of iron complexes. *Coordin. Chem. Rev.* **2018**, *374*, 15–35. [CrossRef]

110. Van der Zee, J.; Krootjes, B.B.; Chignell, C.F.; Dubbelman, T.M.; Van Steveninck, J. Hydroxyl radical generation by a light-dependent Fenton reaction. *Free Radic. Biol. Med.* **1993**, *14*, 105–113.

111. Pozdnyakov, I.P.; Kel, O.V.; Plyusnin, V.F.; Grivin, V.P.; Bazhin, N.M. New insight into photochemistry of ferrioxalate. *J. Phys. Chem. A* **2008**, *112*, 8316–8322. [CrossRef]

112. Nogueira, A.A.; Souza, B.M.; Dezotti, M.W.C.; Boaventura, R.A.R.; Vilar, V.J.P. Ferrioxalate complexes as strategy to drive a photo-FENTON reaction at mild pH conditions: A case study on levofloxacin oxidation. *J. Photoch. Photobio. A* **2017**, *345*, 109–123. [CrossRef]

113. Faust, B.C.; Zepp, R.G. Photochemistry of Aqueous Iron(Iii) Polycarboxylate Complexes—Roles in the Chemistry of Atmospheric and Surface Waters. *Environ. Sci. Technol.* **1993**, *27*, 2517–2522. [CrossRef]

114. Huffman, R.E.; Davidson, N. Kinetics of the Ferrous Iron-Oxygen Reaction in Sulfuric Acid Solution. *J. Am. Chem. Soc.* **1956**, *78*, 4836–4842. [CrossRef]

115. Subelzu, N.; Schöneich, C. Near UV and Visible Light Induce Iron-Dependent Photodegradation Reactions in Pharmaceutical Buffers: Mechanistic and Product Studies. *Mol. Pharm.* **2020**, *17*, 4163–4179. [CrossRef] [PubMed]

116. *Q1B Photostability Testing of New Drug Substances and Products. Guidance for Industry*; International Council for Harmonization (ICH): Geneva, Switzerland, 1996.

117. Zhang, Y.; Richards, D.S.; Grotemeyer, E.N.; Jackson, T.A.; Schöneich, C. Near-UV and Visible Light Degradation of Iron (III)-Containing Citrate Buffer: Formation of Carbon Dioxide Radical Anion via Fragmentation of a Sterically Hindered Alkoxyl Radical. *Mol. Pharm.* **2022**, *19*, 4026–4042. [CrossRef]

118. Koppenol, W.H.; Rush, J.D. Reduction Potential of the Co2/Co2.- Couple—A Comparison with Other C1 Radicals. *J. Phys. Chem.* **1987**, *91*, 4429–4430. [CrossRef]

119. Adams, G.E.; Willson, R.L. Pulse Radiolysis Studies on Oxidation of Organic Radicals in Aqueous Solution. *Trans. Faraday Soc.* **1969**, *65*, 2981. [CrossRef]

120. Fojtik, A.; Czapski, G.; Henglein, A. Pulse Radiolytic Investigation of Carboxyl Radical in Aqueous Solution. *J. Phys. Chem.* **1970**, *74*, 3204. [CrossRef]

121. Willson, R.L. Pulse Radiolysis Studies of Electron Transfer in Aqueous Disulphide Solutions. *J. Chem. Soc. Chem. Comm.* **1970**, *64*, 1425–1426. [CrossRef]

122. Favaudon, V.; Tourbez, H.; Houeelevin, C.; Lhoste, J.M. Co2.- Radical Induced Cleavage of Disulfide Bonds in Proteins—A Gamma-Ray and Pulse-Radiolysis Mechanistic Investigation. *Biochemistry* **1990**, *29*, 10978–10989. [CrossRef]

123. Joshi, R.; Adhikari, S.; Gopinathan, C.; O'Neill, P. Reduction reactions of bovine serum albumin and lysozyme by CO2- radical in polyvinyl alcohol solution: A pulse radiolysis study. *Radiat. Phys. Chem.* **1998**, *53*, 171–176. [CrossRef]

124. Matzapetakis, M.; Raptopoulou, C.P.; Tsohos, A.; Papaefthymiou, V.; Moon, N.; Salifoglou, A. Synthesis, spectroscopic and structural characterization of the first mononuclear, water soluble iron-citrate complex, $(NH_4)_5Fe(C_6H_4O_7)_2 \cdot 2H_2O$. *J. Am. Chem. Soc.* **1998**, *120*, 13266–13267. [CrossRef]

125. Duerkop, M.; Berger, E.; Durauer, A.; Jungbauer, A. Influence of cavitation and high shear stress on HSA aggregation behavior. *Eng. Life Sci.* **2018**, *18*, 169–178. [CrossRef] [PubMed]

126. Duerkop, M.; Berger, E.; Durauer, A.; Jungbauer, A. Impact of Cavitation, High Shear Stress and Air/Liquid Interfaces on Protein Aggregation. *Biotechnol. J.* **2018**, *13*, 1800062. [CrossRef] [PubMed]
127. Nayak, A.; Colandene, J.; Bradford, V.; Perkins, M. Characterization of subvisible particle formation during the filling pump operation of a monoclonal antibody solution. *J. Pharm. Sci.* **2011**, *100*, 4198–4204. [CrossRef]
128. Gikanga, B.; Eisner, D.R.; Ovadia, R.; Day, E.S.; Stauch, O.B.; Maa, Y.F. Processing Impact on Monoclonal Antibody Drug Products: Protein Subvisible Particulate Formation Induced by Grinding Stress. *PDA J. Pharm. Sci. Technol.* **2017**, *71*, 172–188. [CrossRef]
129. Gikanga, B.; Hui, A.; Maa, Y.F. Mechanistic Investigation on Grinding-Induced Subvisible Particle Formation during Mixing and Filling of Monoclonal Antibody Formulations. *PDA J. Pharm. Sci. Technol.* **2018**, *72*, 117–133. [CrossRef]
130. Randolph, T.W.; Schiltz, E.; Sederstrom, D.; Steinmann, D.; Mozziconacci, O.; Schöneich, C.; Freund, E.; Ricci, M.S.; Carpenter, J.F.; Lengsfeld, C.S. Do not drop: Mechanical shock in vials causes cavitation, protein aggregation, and particle formation. *J. Pharm. Sci.* **2015**, *104*, 602–611. [CrossRef]
131. Torisu, T.; Maruno, T.; Hamaji, Y.; Ohkubo, T.; Uchiyama, S. Synergistic Effect of Cavitation and Agitation on Protein Aggregation. *J. Pharm. Sci.* **2017**, *106*, 521–529. [CrossRef]
132. Wu, H.; Chisholm, C.F.; Puryear, M.; Movafaghi, S.; Smith, S.D.; Pokhilchuk, Y.; Lengsfeld, C.S.; Randolph, T.W. Container Surfaces Control Initiation of Cavitation and Resulting Particle Formation in Protein Formulations After Application of Mechanical Shock. *J. Pharm. Sci.* **2020**, *109*, 1270–1280. [CrossRef]
133. Siavashpouri, M.; Bailey-Hytholt, C.M.; Authelin, J.R.; Patke, S. Quantification and Stability Impact Assessment of Drop Stresses in Biologic Drug Products. *PDA J. Pharm. Sci. Technol.* **2022**, *76*, 461–473. [CrossRef]
134. Yasui, K. Production of O Radicals from Cavitation Bubbles under Ultrasound. *Molecules* **2022**, *27*, 4788. [CrossRef] [PubMed]
135. Meyer, B.K.; Ni, A.; Hu, B.; Shi, L. Antimicrobial preservative use in parenteral products: Past and present. *J. Pharm. Sci.* **2007**, *96*, 3155–3167. [CrossRef]
136. Stroppel, L.; Schultz-Fademrecht, T.; Cebulla, M.; Blech, M.; Marhofer, R.J.; Selzer, P.M.; Garidel, P. Antimicrobial Preservatives for Protein and Peptide Formulations: An Overview. *Pharmaceutics* **2023**, *15*, 563. [CrossRef] [PubMed]
137. Sankar, M.; Nowicka, E.; Carter, E.; Murphy, D.M.; Knight, D.W.; Bethell, D.; Hutchings, G.J. The benzaldehyde oxidation paradox explained by the interception of peroxy radical by benzyl alcohol. *Nat. Commun.* **2014**, *5*, 3332. [CrossRef] [PubMed]
138. Grootveld, M.; Halliwell, B. An aromatic hydroxylation assay for hydroxyl radicals utilizing high-performance liquid chromatography (HPLC). Use to investigate the effect of EDTA on the Fenton reaction. *Free Radic. Res. Commun.* **1986**, *1*, 243–250. [CrossRef]
139. Grootveld, M.; Halliwell, B. Aromatic hydroxylation as a potential measure of hydroxyl-radical formation in vivo. Identification of hydroxylated derivatives of salicylate in human body fluids. *Biochem. J.* **1986**, *237*, 499–504. [CrossRef]
140. Maskos, Z.; Rush, J.D.; Koppenol, W.H. The hydroxylation of the salicylate anion by a Fenton reaction and T-radiolysis: A consideration of the respective mechanisms. *Free Radic. Biol. Med.* **1990**, *8*, 153–162. [CrossRef]
141. Hamilton, G.A.; Friedman, J.P.; Campbell, P.M. Hydroxylation of Anisole by Hydrogen Peroxide in Presence of Catalytic Amounts of Ferric Ion and Catechol. Scope Requirements and Kinetic Studies. *J. Am. Chem. Soc.* **1966**, *88*, 5266. [CrossRef]
142. Friedrich, L.C.; Mendes, M.A.; Silva, V.O.; Zanta, C.L.P.S.; Machulek, A.; Quina, F.H. Mechanistic Implications of Zinc(II) Ions on the Degradation of Phenol by the Fenton Reaction. *J. Brazil Chem. Soc.* **2012**, *23*, 1372–1377. [CrossRef]
143. Pasquet, J.; Chevalier, Y.; Pelletier, J.; Couval, E.; Bouvier, D.; Bolzinger, M.A. The contribution of zinc ions to the antimicrobial activity of zinc oxide. *Colloid. Surf. A* **2014**, *457*, 263–274. [CrossRef]
144. Dodson, G.; Steiner, D. The role of assembly in insulin's biosynthesis. *Curr. Opin. Struct. Biol.* **1998**, *8*, 189–194. [CrossRef] [PubMed]
145. Karthikeyan, C.; Arunachalam, P.; Ramachandran, K.; Al-Mayouf, A.M.; Karuppuchamy, S. Recent advances in semiconductor metal oxides with enhanced methods for solar photocatalytic applications. *J. Alloy. Compd.* **2020**, *828*, 154281. [CrossRef]
146. Qin, H.C.; Li, W.Y.; Xia, Y.J.; He, T. Photocatalytic Activity of Heterostructures Based on ZnO and N-Doped ZnO. *ACS Appl. Mater. Inter.* **2011**, *3*, 3152–3156. [CrossRef] [PubMed]
147. Kubo, W.; Tatsuma, T. Photocatalytic remote oxidation with various photocatalysts and enhancement of its activity. *J. Mater. Chem.* **2005**, *15*, 3104–3108. [CrossRef]
148. Al-Rasheed, R.; Cardin, D.J. Photocatalytic degradation of humic acid in saline waters Part 2. Effects of various photocatalytic materials. *Appl. Catal. A Gen.* **2003**, *246*, 39–48. [CrossRef]
149. Parini, R.; Deodato, F. Intravenous Enzyme Replacement Therapy in Mucopolysaccharidoses: Clinical Effectiveness and Limitations. *Int. J. Mol. Sci.* **2020**, *21*, 2975. [CrossRef]
150. Brennan, G.T.; Saif, M.W. Pancreatic Enzyme Replacement Therapy: A Concise Review. *JOP* **2019**, *20*, 121–125.
151. Rivera-Colon, Y.; Schutsky, E.K.; Kita, A.Z.; Garman, S.C. The structure of human GALNS reveals the molecular basis for mucopolysaccharidosis IV A. *J. Mol. Biol.* **2012**, *423*, 736–751. [CrossRef]
152. Demydchuk, M.; Hill, C.H.; Zhou, A.; Bunkoczi, G.; Stein, P.E.; Marchesan, D.; Deane, J.E.; Read, R.J. Insights into Hunter syndrome from the structure of iduronate-2-sulfatase. *Nat. Commun.* **2017**, *8*, 15786. [CrossRef]